Zhou, Y.-L., Li, Y., Luo, D.-M., Wen, C., & Hodgson, P. (2013). Microstructures, mechanical properties and in vitro corrosion behaviour of biodegradable Mg-Zr-Ca alloys.

Originally published in *Journal of Materials Science, 48*(4), 1632–1639.
Available from: http://dx.doi.org/10.1007/s10853-012-6920-2

Microstructures, mechanical properties and in vitro corrosion behaviour of biodegradable Mg-Zr-Ca alloys

Ying-Long Zhou[1,*], Yuncang Li[2,*], Dong-Mei Luo[1], Cuie Wen[3] and Peter Hodgson[2]

[1]*Department of Mechatronics Engineering, Foshan University, Foshan 528000, China*

[2]*Institute for Frontier Materials, Deakin University, Waurn Ponds, VIC 3217, Australia*

[3]*Faculty of Engineering and Industrial Sciences, Swinburne University of Technology, Hawthorn, VIC 3122, Australia*

*Corresponding author. ylzhou@fosu.edu.cn (Y.L Zhou), yuncang.li@deakin.edu.au (Y. C. Li), Tel.: +61 3 5227 2168; fax: +61 3 5227 1103.

Abstract

The microstructures, mechanical properties, corrosion behaviour and biocompatibility of the Mg-Zr-Ca alloys have been investigated for potential use in orthopaedic applications. The microstructures of the alloys were examined using X-ray diffraction analysis，optical microscopy, and scanning electron microscopy. The mechanical properties of Mg-Zr-Ca alloys were determined from compressive tests. The corrosion behaviour has been investigated using an immersion test and electrochemical measurement. The biocompatibility was evaluated by cell growth factor using osteoblast-like SaOS2 cell. The experimental results indicate that the hot-rolled Mg-Zr-Ca alloys exhibit much finer microstructures than the as-cast Mg-Zr-Ca alloys which show coarse microstructures. The compressive strength of the hot-rolled alloys is much higher than that of the as-cast alloys and the human bone, which would offer appropriate mechanical properties for orthopaedic applications. The corrosion resistance of the alloys can be enhanced significantly by hot-rolling process. Hot-rolled Mg-0.5Zr-1Ca alloy (wt.%) exhibits the lowest corrosion rate among all alloys studied in this paper. The hot-rolled Mg-0.5Zr-1Ca and Mg-1Zr-1Ca alloys exhibit better biocompatibility than other studied alloys and possess advanced mechanical properties, corrosion resistance, and biocompatibility, suggesting that they have a great potential to be good candidates for orthopaedic applications.

Keywords: Mg-Zr-Ca alloy; Microstructure; Mechanical property; Corrosion behaviour; Biocompatibility

Introduction

Cobalt-based alloys, stainless steels, and titanium (Ti) alloys have been widely used as hard tissue implants such as plates, screws, and pins for orthopaedic applications [1]. Since these implants are not biodegradable in the human body and may cause long-term complications, a subsequent surgical procedure may be necessary to remove these implants from the human body after the tissues heals. For such applications, it is desirable to use biodegradable implants. Although biodegradable polymeric materials have been used for a long time, these polymeric materials are not suitable to be orthopaedic implants due to their poor mechanical strength. Therefore, it is necessary to develop biodegradable metallic implant materials with appropriate mechanical properties. Magnesium (Mg) and its alloys for biodegradable implants have extensively attracted attentions because they exhibit suitable mechanical properties and can degrade in the human body. The previous studies on using Mg alloys as biomaterials mainly focused on Mg-Al and Mg-RE alloy systems [2-4] and the existing Mg and its alloys corrode rapidly in the human body fluid [3-5]. It can result in loss of mechanical integrity before the tissue heals and hydrogen production near the implants, which retard the healing process [3, 5]. Hence, it is necessary to develop novel biodegradable Mg alloys that would corrode at acceptably low rates to ensure Mg alloy implants with the function of loading-bearing through their service lives and reduce hydrogen bubbles in the healing process.

Element alloying is an effective method to enhance corrosion resistance. Zinc (Zn), manganese (Mn), calcium (Ca) and rare earth elements (RE) are regarded as suitable alloying elements for the development of biodegradable Mg alloys [5]. So

far, some Mg alloys such as Mg-Zn, Mg-Zn-Mn, Mg-Zn-Mn-Ca, Mg-Zn-Y, Mg-Si-Ca-Zn, and Mg-Ca alloys have been studied for biomedical applications [6-12]. Other than Zn and aluminium (Al), zirconium (Zr) is also a very effective alloying element in improving both the corrosion resistance and strength in Al-free Mg alloys [3, 13-14], though it has been reported that the presence of Zr is associated with some illnesses [5]. However, recent studies [13. 15] have verified the biocompatibility of Mg alloys with a small amount of Zr, hence the Mg-Zr based alloys with low Zr content may be promising candidates for biomedical applications. Up until now, there are a few reports on biomedical Mg-Zr based alloys [13, 15-16]. In this study, Mg-Zr based alloys were chosen as an experimental model to screen for the potential use in biomedical applications. Since Ca is an essential element in the human body and a minor addition of Ca (below 2 wt.%) can enhance the corrosion resistance of Mg alloys [12-13], it has also been chosen as an alloying element. To the best knowledge of the authors, Mg-Zr-Ca alloys have not been systematically studied for orthopaedic applications.

Experimental and methods

The designed Mg-Zr-Ca alloys such as Mg-0.5Zr-1Ca, Mg-0.5Zr-2Ca, Mg-1Zr-1Ca, and Mg-1Zr-2Ca alloys (wt. %, hereafter) were fabricated from commercial pure Mg (99.9%), Ca (99.9%), and master Mg-33Zr alloy. The obtained ingots were homogenized at 450 ^{o}C for 18 ks, hot-rolled by the same thickness reduction and quenched rapidly in ice water.

The phase constitution of the alloys was determined using X-ray diffraction (XRD) analysis. For metallographic observation, the specimens were examined using optical microscopy (OM) and scanning electron microscopy (SEM)

equipped with an energy dispersive spectroscopy (EDS) after they were ground with SiC emery papers of up to 3000 grit, polished with 0.5 μm diamond powder, and then etched with a dilute solution of 10 vol.% nitric acid and 90 vol.% methanol.

The compressive samples (25 mm in gauge length, 10 mm in width, and 10 mm in thickness) were machined from the hot-rolled plates along the rolling direction. The compressive tests were conducted at a crosshead speed of 0.0025 mm/s at room temperature using an Instron machine. The compressive properties such as compressive strength (CS), compressive yield strength (CYS), and compressive modulus of elasticity (CM) were obtained based on the average result of three tests.

Cubed samples with a dimension of 10 mm x 10 mm x 10 mm were cut from the ingots and hot-rolled plates. All samples were ground with SiC emery papers of up to 1500 grit and finely polished with 0.5 μm diamond powder, then cleaned in distilled water and ethanol, and weighed after drying in warm flowing air. The samples were immersed in 200 ml Hank's solution at 37 ± 1 ^{o}C for 15 day. The pH of the solution was adjusted to 7.4 with NaOH or HCl solution before experiment. After the tests, the samples were cleaned by chromic acid (150 g/l) for 10 mins to remove the corrosion products on the surfaces and then were weighed again after washing with ethanol and drying in warm flowing air. A mean of corrosion weight loss for each alloy was obtained by measuring three samples. The corrosion rate was calculated by the weight loss per surface area per day.

Disc samples with a diameter of 9 mm and thickness of 2 mm were used for the electrochemical test. All samples were connected to a copper wire and then mounted in epoxy resin with only an exposed area of 0.64 cm^2 parallel to the

rolling direction as the working electrode. Before the electrochemical test, the mounted sample was successively polished with 240, 600 and 1200-grit sand papers, then carefully degreased with acetone, ethanol and rinsed with distilled water, and lastly dried in a stream of warm air. The open circuit potential and potentiodynamic polarization curve of samples soaked in simulative body fluid (SBF) [17] were measured by an electrochemical station (1470E Multichannel Potentiostat, Solartron, UK) equipped with Multistate software. The SBF of 1 litre was prepared by dissolving the following chemicals in the sequence of NaCl (5.403 g), $NaHCO_3$ (0.504 g), Na_2CO_3 (0.426 g), KCl (0.225 g), $K_2HPO_4 \cdot 3H_2O$ (0.230 g), $MgCl_2 \cdot 6H_2O$ (0.311 g), $CaCl_2$ (0.293 g), and Na_2SO_4 (0.072 g). The solution was buffered to pH 7.40 with HEPES and 1 M NaOH at 37 °C. All experiments were carried out in a thermostat at the temperature of 37 ^{o}C. A three-electrode cell system with a saturated calomel electrode (SCE), a 1.5 x 1.5 cm^2 platinum electrode and the sample mounted in epoxy resin as the reference electrode, the counter electrode and the working electrode used in this study. Before measurements, the working electrode was immersed in test solution for stability. The corrosion density current (I_{corr}) and corrosion rate were calculated using CView software.

Osteoblast-like cells (SaOS2), a human osteosarcoma cell line with osteoblastic properties [18], were cultured in a modified minimum essential media (MMEM) at 37 °C in a humidified atmosphere of 5 % CO_2 in air. MMEM is composed of minimum essential media (Gibco, Invitrogen, Mulgrave, VIC, Australia) supplemented with 10 % fetal bovine serum (Bovogen Biologicals, Essendon, VIC, Australia), 1 % non-essential amino acid (Sigma-Aldrich, Castle Hill, NSW, Australia), 10,000 units/mL penicillin-10,000 μg/mL streptomycin (Gibco), and 0.4 % amphostat B (In Vitro Technologies, Auckland, New

Zealand). The culture medium was changed every 3 days. When cells confluence, cells were harvested using 0.1 % Trypsin-5 mM EDTA (Sigma-Alrdrich, Australia) and collected for use.

SaOS2 cells were used to evaluate the biocompatibility of Mg-Zr-Ca alloys by the indirect contact method [13, 19] according to ISO 10993-5 [20]. Extracts were prepared using MMEM with a surface area to MMEM ratio of 0.6 cm^2/ ml in a humidified atmosphere with 5 % CO_2 at 37 ^oC for 72 h. The supernatant fluid was withdrawn and filter-sterilized with a 0.22-μm filter (Falcon, BD Biosciences, San Jose, CA, USA) to obtain the extracts. The control groups involved the use of MMEM medium as negative controls.

SaOS2 cells were mixed with MMEM at a cell density of 5 x 10^4 cells/ml. A mixture of 200 μl was transferred into a well of 48-well cell culture plate. The cell culture plate was placed in an incubator at a humidified atmosphere with 5 % CO_2 at 37 ^oC for 24 h to allow cells attachment. The MMEM in each well was then sucked out and an extracts of 200 μl was refilled in each well. After further incubation of the cells in a humidified atmosphere with 5 % CO_2 at 37 ^oC for 24 h, the 48-well cell culture plates were observed under an optical microscope. After that, a MTS (3-(4,5-dimethylthiazol-2-yl)-5-(3-carboxymethoxyphenyl)-2-(4-sulfophenyl)-2H-tetrazolium) assay, a colorimetric assay was used to measure the cell number in each well. The MTS measurement processes are briefly as follows. The extract in each well was replaced by 150 μl phenol red free media. 50 μl MTS/PMS solution was added to each well and the cell culture plate was incubated for 1 h at 37 ^oC with 5 % CO_2. Then, 100 μl of the solution from each well was transferred to a 96 well plate for absorbance reading at 490 nm using a spectrophotometer (GENios Pro, Tecan, Mannedorf, Switzerland). The growth

factor of the cells on the Mg alloys was defined as the ratio of live cell number in extraction media to that of the control.

Results and discussion

The XRD patterns of hot-rolled Mg-Zr-Ca alloys are shown in Fig 1. It can be observed that the strongest peak for all the hot-rolled alloys is (002) while that of as-cast pure Mg is (102), which is related to the rolling texture. The Mg-Zr-Ca alloys with 1 % Ca are composed of a single α phase while those with 2 % Ca consist of both a Mg_2Ca and an α phase. The formation of Mg_2Ca in the Mg-0.5Zr-2Ca and Mg-1Zr-2Ca alloys is related to the limited solubility of Ca in Mg [13-14, 21], which is in agreement with the results of previous investigations [11–13].

The OM microstructures of as-cast alloys are shown in Fig. 2. As-cast alloys exhibit coarse microstructures with large grain sizes. It can be observed that the Mg-1Zr-1Ca alloy exhibits the finest microstructure (Fig. 2(c)) among them. Mg-Zr-Ca alloys with 2 % Ca show coarse grain boundaries as shown in Figs. 2(b) and (d). In order to characterize the coarse grain boundaries, SEM technique was employed. Figure 3 shows the high magnification image of the Mg-0.5Zr-2Ca alloy. The EDS result indicates that the compositions of Mg, O and Ca in the coarse boundary (rectangular box in Fig.3) of the Mg-0.5Zr-2Ca alloy are 67.07, 26.19 and 6.74 wt. %, respectively. It can be observed that Ca content is rich in the grain boundary, which suggests that the Mg_2Ca precipitates along the grain boundaries. This is in agreement with the previous study since Mg_2Ca preferentially precipitates along the grain boundaries of the Mg alloys [11]. Zr has not been detected by EDS on the grain boundary of the Mg-0.5Zr-2Ca alloy, which may be related to the fact that Zr with similar crystal parameters to α-Mg

and much higher melting point than the other elements usually acts as the centre of heterogeneous nucleation (α-Mg) in Mg-Zr based alloys during the solidification [14, 21].

Figures 4 and 5 show the microstructures of longitudinal sections and cross-sections, respectively, of the hot-rolled Mg-Zr-Ca alloys. Compared to the microstructures of as-cast alloys, the hot-rolled alloys exhibit much finer structures. In the microstructure of the longitudinal section (Fig. 4), a typical elongated grain structure is observed, which is caused by the hot-rolling process. In the cross-section microstructure (Fig. 5), a typical equiaxed microstructure is observed in all the alloys. The relatively coarser grain boundaries are also related to the formation of Mg_2Ca, as shown in figure 2.

For potential biodegradable implants, the compressive properties are more important than tensile properties. The compressive properties of Mg-Zr-Ca alloys were measured as shown in Fig. 6. It can be observed from Fig. 6(a) that the compressive yield strength of all the as-cast alloys is much higher than that of pure Mg (60~100 MPa) [3] due to the solid strengthening from both Zr and Ca. The Mg-1Zr-1Ca alloy exhibits the highest compressive strength among them, which is related to it having the finest microstructure (Fig.2 (c)). The compressive moduli of elasticity for the alloys are similar, which indicates that the compressive modulus of the alloys is not sensitive to Zr and Ca content. However, the compressive strength of as-cast alloys is only at the level of the natural bone (130~180 MPa) [3], therefore these as-cast alloys are not strong enough for biomedical applications.

It can be observed in Fig. 6(b) that the compressive yield strength of the alloys has been improved considerably after hot-rolling, and is much higher than that of the human bone [3]. Therefore these hot-rolled alloys offer good

mechanical properties for orthopaedic applications. It is considered that the enhanced mechanical properties of the alloys are related to finer microstructures and rolling texture. There is a significant difference in strength when compared to the as-cast alloys, which indicates the different solid solution strengthening effects of Zr and Ca. However, the hot-rolled alloys show similar compressive strengths to one another, which implies that the strengthening effect of hot-rolling is much stronger than that of the solid solution strengthening. The as-cast Mg-1Zr-1Ca alloy has the highest compressive strength among the as-cast alloys, which indicates that it has the strongest solid strengthening effect from Zr and Ca. This helps us understand why the hot-rolled Mg-1Zr-1Ca alloy exhibits the highest strength among all the hot-rolled alloys since the same hot-rolling process should cause the same work hardening effect on all the alloys. The hot-rolled alloys exhibit slightly higher compressive moduli than the corresponding as-cast alloys, which is related to the plastic deformation such as rolling process usually brings about the texture as shown in Fig. 1 and results in elastic anisotropy [22-25] in spite of the same chemical composition and constituent phase.

The corrosion rate of the alloys immersed in Hank's solution for 15 days is shown in Fig. 7(a). It reveals that all as-cast Mg-Zr-Ca alloys exhibit lower corrosion rate than commercially pure Mg (19 ~ 44 $mg/cm^2/day$) [5], which indicates that the addition of Zr and Ca to Mg can improve its corrosion resistance. During the immersion tests, the white corrosion products were kept precipitating at the bottom of the beakers. The pH of the corrosion solution gradually changed from 7.4 to 9.2 during the soaking, showing strong alkalization during the tests. Fig. 7(b) and Table 1 show the corrosion rate and corrosion current density (I_{corr}) of the alloys immersed in SBF at 37 ^{o}C, which was calculated from the polarization curves of the alloys in SBF (shown in Fig. 8). The

results of the immersion test and the electrochemical measurement indicate that the as-cast and hot rolled alloys with 2 % Ca have a higher corrosion rate and I_{corr} than those with 1 % Ca (shown in Fig. 7 and Table 1). In as-cast alloys, the Mg-1Zr-1Ca alloy showed the lowest corrosion rate and I_{corr}. After the hot-rolling process, the corrosion resistance of the alloys had been enhanced significantly. This is associated with the reduced microscopic segregation, decreased cast deflects, and finer microstructures caused by the hot-rolling process. It is considered that the as-cast microscopic segregation and cast deflects of metallic materials accelerate the corrosion [26-29] and fine grains can create more grain boundaries that act as corrosion barriers and accordingly enhance the corrosion resistance of Mg alloys [30-33]. The as-cast and hot-rolled alloys with 2 % Ca show coarser grain boundary than those with 1 % Ca (Figs. 3, 4 and 5), indicating that the great volume of intermetallic Mg_2Ca phase resides in the grain boundary, which reduces the corrosion resistance of those alloys with 2 % Ca. This result is in agreement with the previous study [12].

The biocompatibility of the biodegradable magnesium alloys can be affected by the corrosion resistance significantly [2, 34]. Better corrosion resistance is expected to achieve better biocompatibility. Since hot-rolled Mg-0.5Zr-1Ca and Mg-1Zr-1Ca alloys show much better corrosion behaviour, their biocompatibility was carried out using SaOS2 cell. To investigate the effect of hot rolling on the biocompatibility, the as-cast Mg-0.5Zr-1Ca and Mg-1Zr-1Ca alloys were selected to do the biocompatibility test. Figure 9 shows the cell growth factor of the as-cast and hot-rolled Mg-Zr-Ca alloys with 1 % Ca. It is noticeable that Mg-0.5Zr-1Ca and Mg-1Zr-1Ca alloys in both as-cast and hot-rolled form displayed high cell growth factors (the negative control group regarded as biocompatible has the cell growth factor of 1). This indicates that they are biocompatible. The Mg-0.5Zr-1Ca

alloy in both as-cast and hot-rolled form exhibits higher cell growth factor than that of the Mg-1Zr-1Ca alloy in both as-cast and hot-rolled form. After hot-rolling process, the biocompatibility of the alloys has been enhanced, which is of benefit to better corrosion resistance of the alloys.

Conclusions

The microstructures, compressive properties, corrosion resistance, and biocompatibility of Mg-Zr-Ca alloys have been investigated. The following conclusions can be obtained.

1) The hot-rolled Mg-Zr-Ca alloys exhibit much finer microstructures than the as-cast alloys.

2) The hot-rolled Mg-Zr-Ca alloys have much higher compressive strength than the as-cast alloys and the human bone, and offer good mechanical properties for orthopaedic applications.

3) The hot-rolling process significantly enhances corrosion resistance of the Mg-Zr-Ca alloys. The hot-rolled Mg-0.5Zr-1Ca alloy has the slowest corrosion rate among all the studied alloys.

4) Among all the alloys, the hot-rolled Mg-0.5Zr-1Ca and Mg-1Zr-1Ca alloys possess advanced mechanical properties, corrosion resistance and biocompatibility, suggesting that they have a great potential to be good candidates for biomedical applications.

Acknowledgements

This work was financially supported by the funds of the Key Scientific and Technological Projects of Guangdong Province, PR China (2008B010600003) and AISRF-BF030031, Australia.

References

1. Long M, Rack HJ (1998) Biomaterials 19:1621
2. Witte F, Fischer J, Nellesen J, Crostack H-A, Kaese V, Pisch A, et al. (2006) Biomaterials 27:1013
3. Staiger MP, Pietak AM, Huadmai J, Dias G (2006) Biomaterials 27:1728.
4. Witte F, Kaese V, Haferkamp H, Switzer E, Meyer-Lindenberg A, Wirth CJ, et al. (2005) Biomaterials 26:3557
5. Song G (2007) Corr Sci 49:1696
6. Zhang S, Zhang X, Zhao C, Li J, Song Y, Xie C, Tao H, Zhang Y, He Y, Jiang Y, Bian Y (2010) Acta Biomater 6:626
7. Zhang E, Yin D, Xu L, Yang L, Yang K. (2009) Mater Sci Eng C 29:987
8. Zhang E, Yang L (2008) Mater Sci Eng A 497:111
9. Zhang E, He W, Dui H, Yang K (2008) Mater Sci Eng A 488:1021
10. Zhang E, Yang L, Xu J, Chen H (2010) Acta Biomater 6:1756
11. Li Z, Gu X, Lou S, Zheng Y (2008) Biomaterials 29:1329
12 Wan Y, Xiong G, Luo H, He F, Huang Y, Zhou X (2008) Mater & Design 29:2034
13. Gu X, Zheng Y, Cheng Y, Zhong S, Xi T (2009) Biomaterials 30:484
14. Xu H, Liu JA, Xie SS (2007) Magnesium alloys fabrication and processing technology China, Metallurgical Industry Press, Beijing, China
15. Ye XY, Chen MF, Yang M, Wei J, Liu DB (2010) J Mater Sci: Mater Med 21:1321
16. Tsai MH, Chen MS, Lin LH, Lin MH, Wu CZ, Ou KL, Yu CH (2011) J Alloys and Compd 21: 813
17. Li Y, Hodgson P, Wen C (2011) J Mater Sci 46:365
18. Rodan SB, Imai Y, Thiede MA, Wesolowski G, Thompson D, Bar-Shavit Z, et al. (1987) Cancer Res 47:496
19. Li Y, Wong C, Xiong J, Hodgson P, Wen C (2010) J Dent Res 89:493.
20. International organization for Standardization (1999) Biological evaluation of medical devices. ISO10993-5. ANSI/AAMI, Arlington
21. International. A. ASM Handbook (1992) 03: Alloy Phase Diagrams. ASM International, USA
22. Zhou Y-L, Luo D-M (2011) Mater Character 62:931
23. Matsumoto H, Watanabe S, Hanada S (2007) J Alloy Compd 439:146

24. Collings EW. (1984) The physical metallurgy of titanium alloys. Metals Park, OH: ASM International, USA
25. Cui ZX (2000) Metallography and heat treatments. Mechanical Industry Press, Beijing, China
26. ASM International Handbook Committee ASM Handbook (1987) Corrosion vol. 13. Materials Park: ASM International, USA
27. Davis JR (2000) Corrosion Understanding the basics. Materials Park: ASM International; USA
28. Laque FL, Copson HR (1963) Corrosion resistance of metals and alloys. Reinhold Publishing Corporation, New York
29. Shreir LL (1963) Corrosion vol. 1: Corrosion of metals and alloys. George Newnes Ltd, London
30. Zhang X, Yuan G, Mao L, Niu J, Fu P, Ding W (2012) J Mech Behav Biomed Mater 7:77
31. Alvarez-Lopez M, Pereda MD, Del Valle JA, Fernandez-Lorenzo M, Garcia-Alonso MC, Ruano OA, et al. (2010) Acta Biomater 6:1763
32. Hamu GB, Eliezer D, Wagner L (2009) J Alloy Compd 468:222
33. Liu C, Xin Y, Tang G, Chu PK (2007) Mater Sci Eng A 456:350
34. Witte F (2010) Acta Biomater 6:1680

Captions for Tables and Figures

Table 1 Corrosion current density of the as-cast and hot rolled Mg-Zr-Ca alloys in SBF

Fig. 1 XRD patterns of hot-rolled Mg-Zr-Ca alloys and as-cast pure Mg

Figure 2 OM microstructures of as-cast Mg-Zr-Ca alloys

Fig. 3 SEM micrograph of the as-cast Mg-0.5Zr-2Ca alloy

Fig. 4 OM microstructures of the longitudinal sections of hot-rolled Mg-Zr-Ca alloys

Fig. 5 OM microstructures of the cross-sections of hot-rolled Mg-Zr-Ca alloys

Fig. 6 Compressive properties of (a) as-cast and (b) hot-rolled Mg-Zr-Ca alloys

Fig. 7 Corrosion rate of the Mg-Zr-Ca alloys immersed in (a) Hank's solution for 15 days by weight loss and (b) SBF by electrochemical measurement (MPY: the unit of corrosion rate, 1MPY = 0.0121 mg/cm^2/day for Mg-Zr-Ca alloys)

Fig. 8 Polarization curves in SBF of the as-cast and hot-rolled alloys□(a) Mg-0.5Zr-1Ca and Mg-1Zr-1Ca (b) Mg-0.5Zr-2Ca and Mg-1Zr-2Ca

Fig. 9 Cell growth factor of Mg-0.5Zr-1Ca and Mg-1Zr-1Ca alloys

Table 1

Alloys	I_{corr} (as-cast, x10^{-3} A/cm^2)	I_{corr} (hot-rolled, x10^{-4} A/cm^2)
Mg-0.5Zr-1Ca	1.30 ± 0.18	1.51 ± 0.15
Mg-1Zr-1Ca	0.43 ± 0.07	2.26 ± 0.19
Mg-0.5Zr-2Ca	1.77 ± 0.20	6.94 ± 0.26
Mg-1Zr-2Ca	1.50 ± 0.16	4.27 ± 0.17

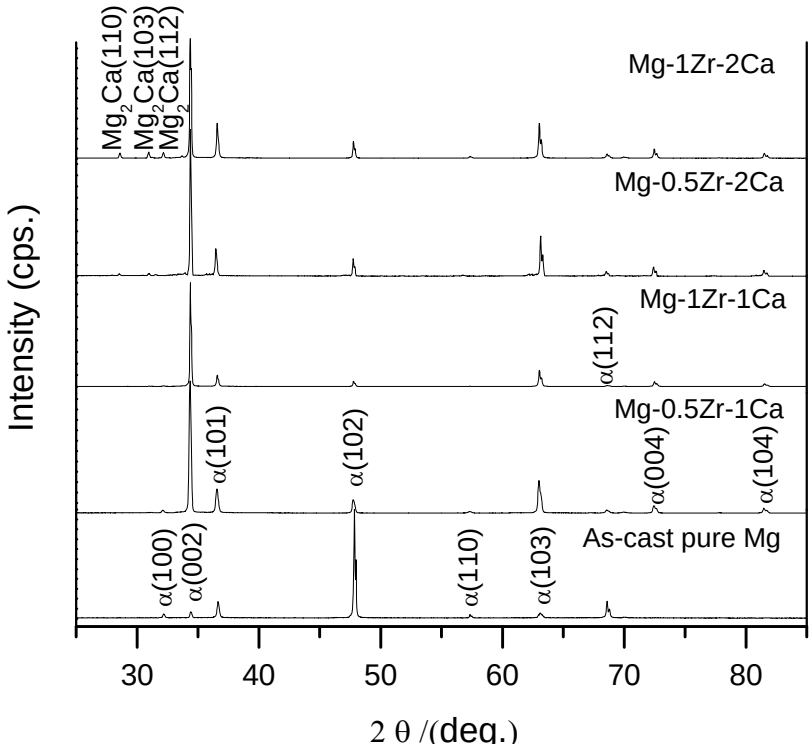

Fig. 1

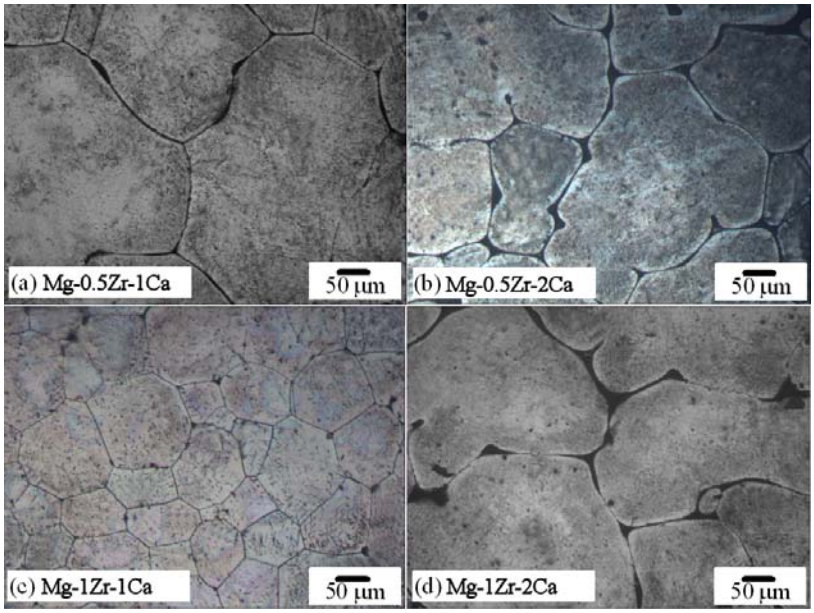
(a) Mg-0.5Zr-1Ca
50 μm
(b) Mg-0.5Zr-2Ca
50 μm
(c) Mg-1Zr-1Ca
50 μm
(d) Mg-1Zr-2Ca
50 μm

Fig. 2

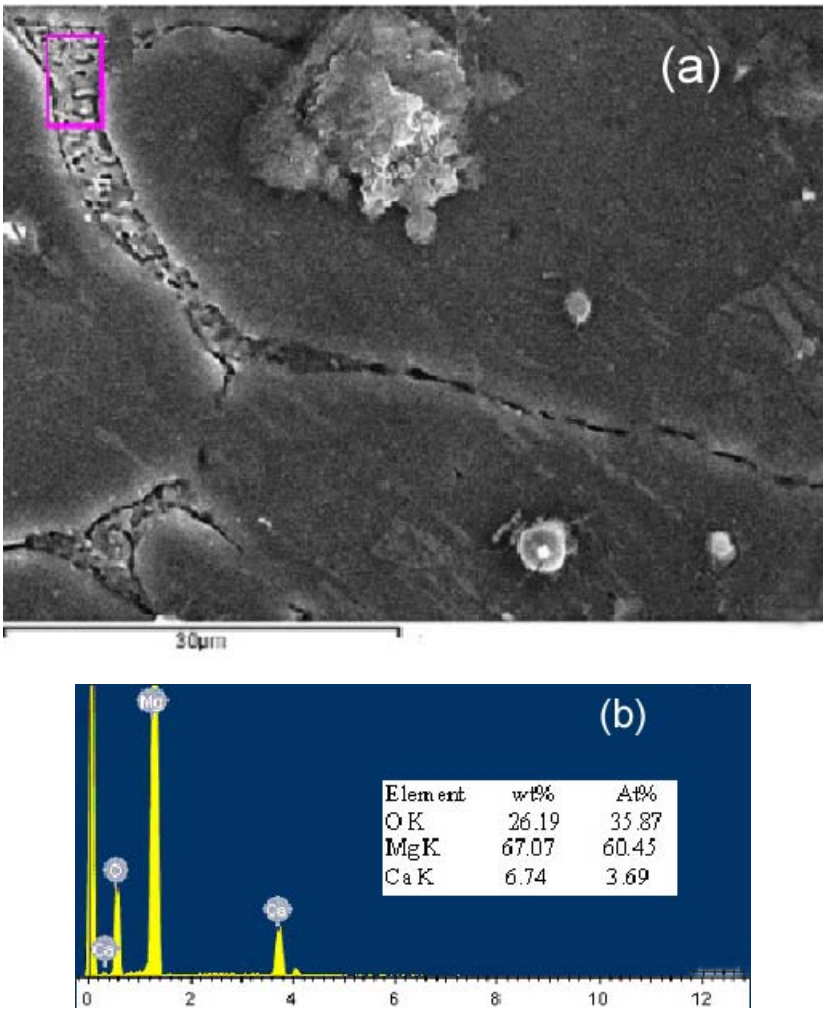
(a)
30μm
(b)
Element wt% At%
O K 26.19 35.87
Mg K 67.07 60.45
Ca K 6.74 3.69
Mg
Ca
0
2
4
6
8
10
12

Fig. 3

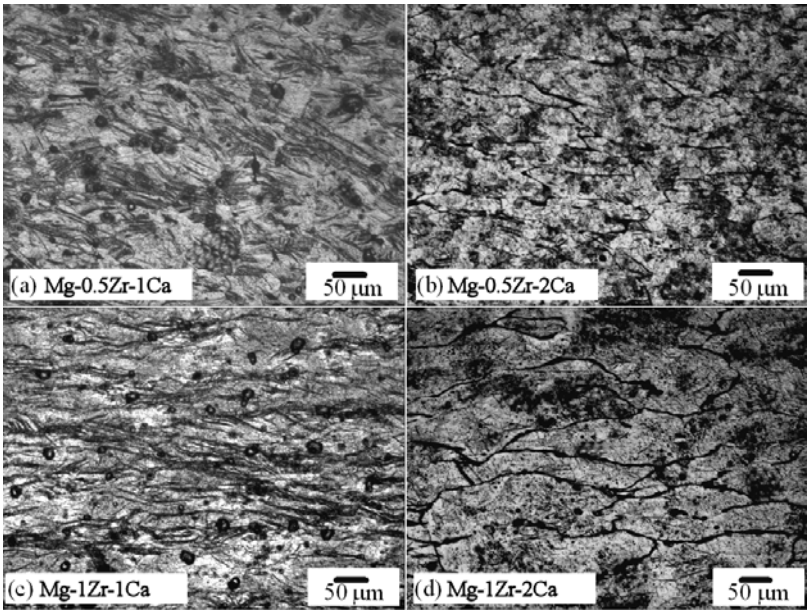
(a) Mg-0.5Zr-1Ca
50 μm
(b) Mg-0.5Zr-2Ca
50 μm
(c) Mg-1Zr-1Ca
50 μm
(d) Mg-1Zr-2Ca
50 μm

Fig. 4

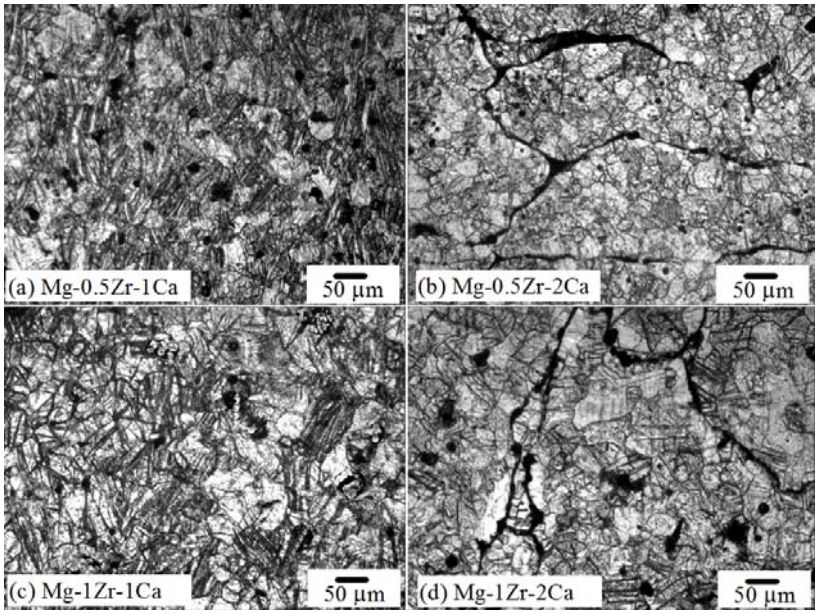
(a) Mg-0.5Zr-1Ca
50 μm
(b) Mg-0.5Zr-2Ca
50 μm
(c) Mg-1Zr-1Ca
50 μm
(d) Mg-1Zr-2Ca
50 μm

Fig. 5

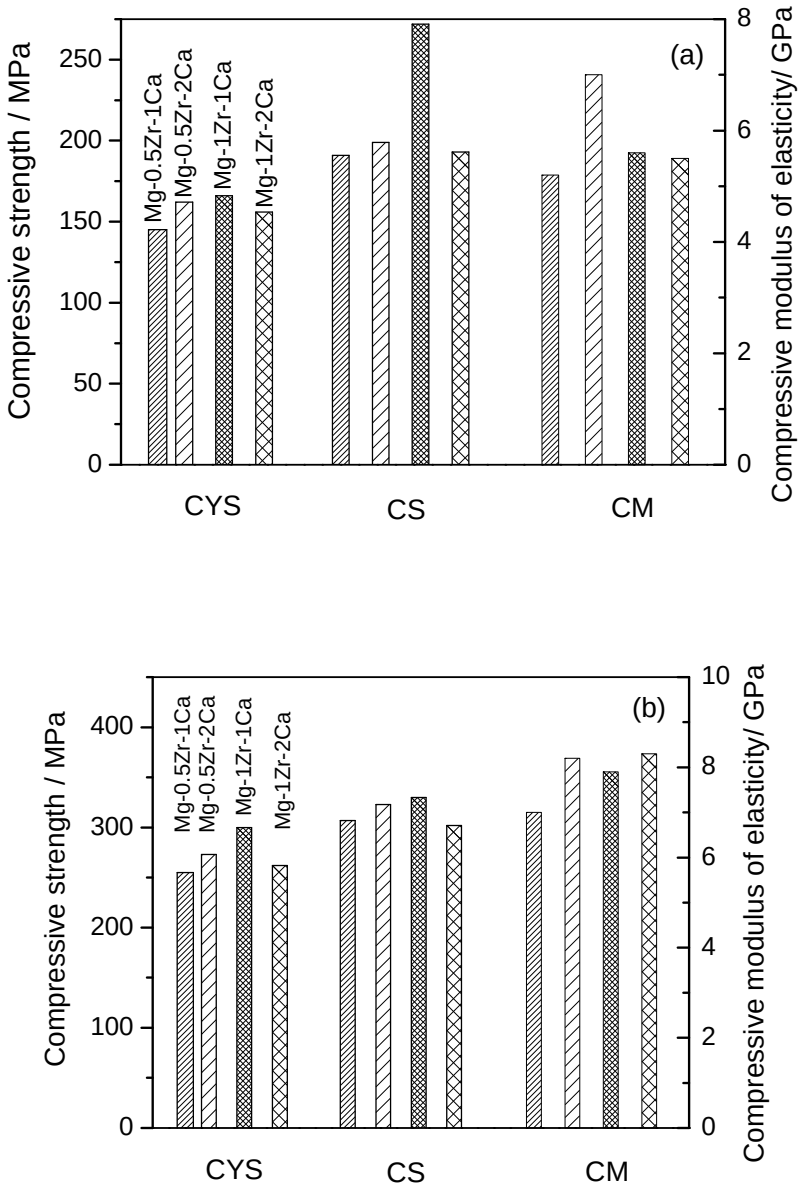
(a)
Compressive strength / MPa
Compressive modulus of elasticity/ GPa
Mg-0.5Zr-1Ca
Mg-0.5Zr-2Ca
Mg-1Zr-1Ca
Mg-1Zr-2Ca
0
50
100
150
200
250
0
2
4
6
8
CYS
CS
CM
(b)
Compressive strength / MPa
Compressive modulus of elasticity/ GPa
Mg-0.5Zr-1Ca
Mg-0.5Zr-2Ca
Mg-1Zr-1Ca
Mg-1Zr-2Ca
0
100
200
300
400
0
2
4
6
8
10
CYS
CS
CM

Fig. 6

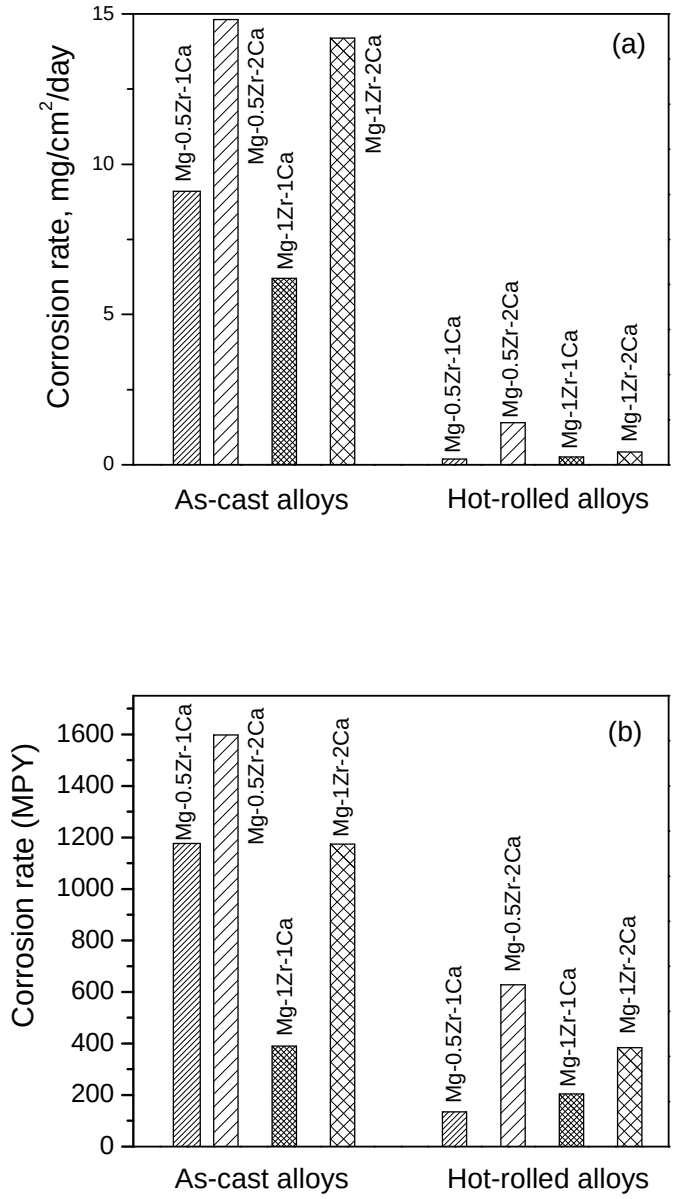
(a)
Corrosion rate, mg/cm^2/day
15
10
5
0
Mg-0.5Zr-1Ca
Mg-0.5Zr-2Ca
Mg-1Zr-1Ca
Mg-1Zr-2Ca
Mg-0.5Zr-1Ca
Mg-0.5Zr-2Ca
Mg-1Zr-1Ca
Mg-1Zr-2Ca
As-cast alloys
Hot-rolled alloys
(b)
Corrosion rate (MPY)
1600
1400
1200
1000
800
600
400
200
0
Mg-0.5Zr-1Ca
Mg-0.5Zr-2Ca
Mg-1Zr-1Ca
Mg-1Zr-2Ca
Mg-0.5Zr-1Ca
Mg-0.5Zr-2Ca
Mg-1Zr-1Ca
Mg-1Zr-2Ca
As-cast alloys
Hot-rolled alloys

Fig. 7

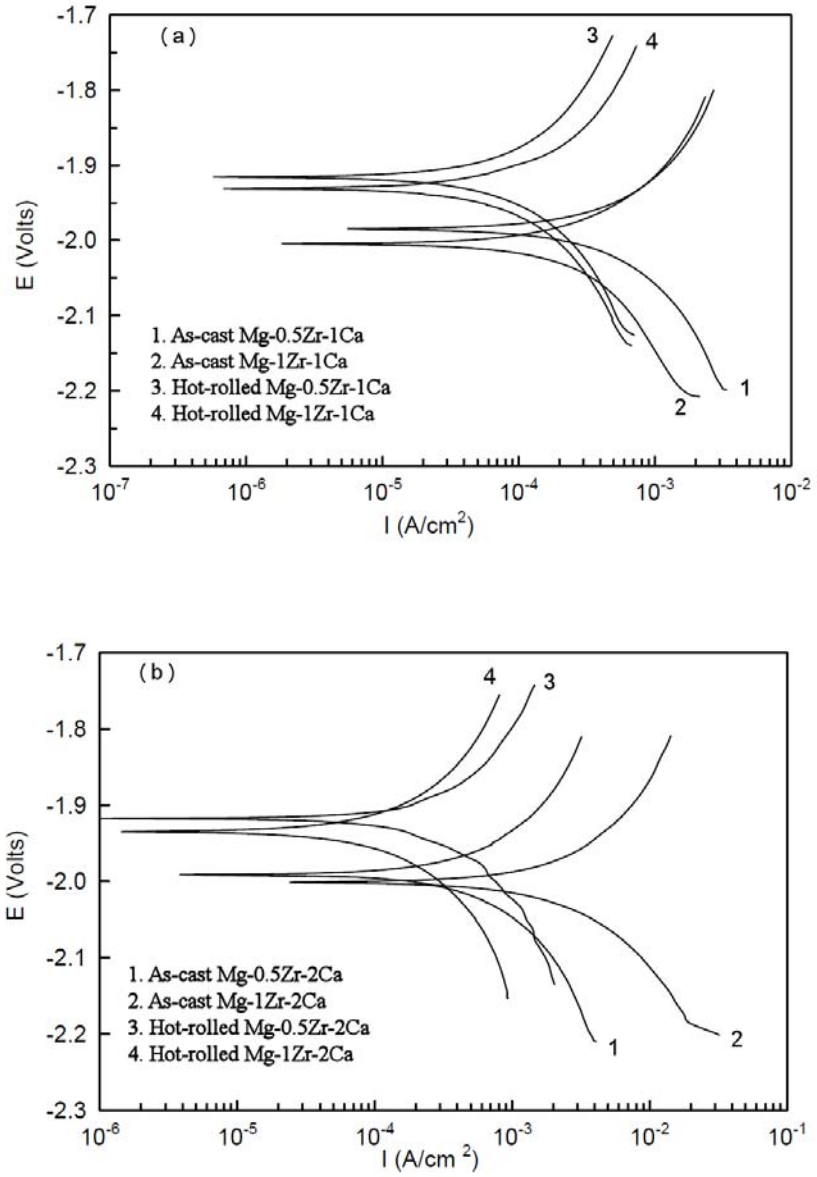
(a)
(b)
E (Volts)
I (A/cm²)
I (A/cm ²)
1. As-cast Mg-0.5Zr-1Ca
2. As-cast Mg-1Zr-1Ca
3. Hot-rolled Mg-0.5Zr-1Ca
4. Hot-rolled Mg-1Zr-1Ca
1. As-cast Mg-0.5Zr-2Ca
2. As-cast Mg-1Zr-2Ca
3. Hot-rolled Mg-0.5Zr-2Ca
4. Hot-rolled Mg-1Zr-2Ca

Fig. 8

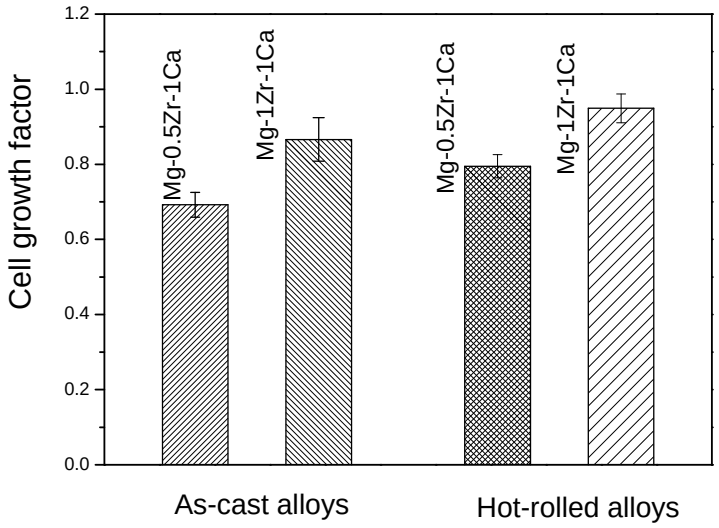
Cell growth factor
1.2
1.0
0.8
0.6
0.4
0.2
0.0
Mg-0.5Zr-1Ca
Mg-1Zr-1Ca
Mg-0.5Zr-1Ca
Mg-1Zr-1Ca
As-cast alloys
Hot-rolled alloys

Fig. 9